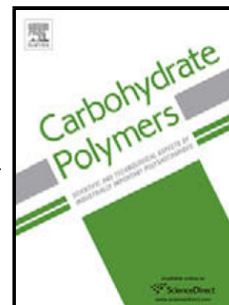


# Journal Pre-proof

ER-Golgi dynamics of HS-modifying enzymes via vesicular trafficking is a critical prerequisite for the delineation of HS biosynthesis



Maria C.Z. Meneghetti (Methodology) (Investigation) (Writing - original draft) (Writing - review and editing), Paula Deboni (Investigation), Carlos M.V. Palomino (Investigation), Luiz P. Braga (Investigation), Renan P. Cavalheiro (Investigation), Gustavo M. Viana (Investigation), Edwin A. Yates (Conceptualization) (Writing - review and editing) (Supervision), Helena B. Nader (Methodology) (Writing - review and editing) (Resources) (Supervision) (Funding acquisition), Marcelo A. Lima (Conceptualization) (Methodology) (Writing - review and editing) (Resources) (Supervision) (Project administration) (Funding acquisition)

PII: S0144-8617(20)31650-7

DOI: <https://doi.org/10.1016/j.carbpol.2020.117477>

Reference: CARP 117477

To appear in: *Carbohydrate Polymers*

Received Date: 19 October 2020

Revised Date: 27 November 2020

Accepted Date: 30 November 2020

Please cite this article as: Meneghetti MCZ, Deboni P, Palomino CMV, Braga LP, Cavalheiro RP, Viana GM, Yates EA, Nader HB, Lima MA, ER-Golgi dynamics of HS-modifying enzymes via vesicular trafficking is a critical prerequisite for the delineation of HS biosynthesis, *Carbohydrate Polymers* (2020), doi: <https://doi.org/10.1016/j.carbpol.2020.117477>

This is a PDF file of an article that has undergone enhancements after acceptance, such as the addition of a cover page and metadata, and formatting for readability, but it is not yet the definitive version of record. This version will undergo additional copyediting, typesetting and review before it is published in its final form, but we are providing this version to give early visibility of the article. Please note that, during the production process, errors may be discovered which could affect the content, and all legal disclaimers that apply to the journal pertain.

© 2020 Published by Elsevier.

## **ER-Golgi dynamics of HS-modifying enzymes via vesicular trafficking is a critical prerequisite for the delineation of HS biosynthesis**

Maria C.Z. Meneghetti<sup>1</sup>, Paula Deboni<sup>1</sup>, Carlos M.V. Palomino<sup>1</sup>, Luiz P. Braga<sup>1</sup>, Renan P. Cavalheiro<sup>1</sup>, Gustavo M. Viana<sup>1</sup>, Edwin A. Yates<sup>2,1</sup>, Helena B. Nader<sup>1</sup> and Marcelo A. Lima<sup>3,1\*</sup>

<sup>1</sup>Departamento de Bioquímica, Instituto de Farmacologia e Biologia Molecular, Escola Paulista de Medicina, Universidade Federal de São Paulo, Rua Três de Maio, 100 – São Paulo, SP, 04044-020, Brazil

<sup>2</sup>Department of Biochemistry and Systems Biology, ISMB, University of Liverpool, Liverpool, Liverpool L69 7ZB, UK

<sup>3</sup>Molecular & Structural Biosciences, School of Life Sciences, Keele University, Huxley Building, Keele, Staffordshire ST5 5BG, UK

### **\*Corresponding author:**

Marcelo A. Lima

Molecular & Structural Biosciences, School of Life Sciences, Keele University, Huxley Building, Keele, Staffordshire ST5 5BG, UK

Email address: m.andrade.de.lima@keele.ac.uk (M A. Lima)

Phone numbers: 01782734111

## Highlights

- HS-modifying enzymes are actively engaged in both anterograde and retrograde Golgi transport;
- HS-modifying enzymes are sorted and trafficked by similar mechanisms;
- BFA treatment changed HS-modifying enzymes vesicular trafficking;
- HS-modifying enzymes moved from cis to trans-Golgi during heparin stimulus;
- Changes in the localization of HS-modifying enzymes correlate with changes in HS structure.

## Abstract

The cell surface and extracellular matrix polysaccharide, heparan sulfate (HS) conveys chemical information to control crucial biological processes. HS chains are synthesized in a non-template driven process mainly in the Golgi apparatus, involving a large number of enzymes capable of subtly modifying its substitution pattern, hence, its interactions and biological effects. Changes in the localization of HS-modifying enzymes throughout the Golgi were found to correlate with changes in the structure of HS, rather than protein expression levels. Following BFA treatment, the HS-modifying enzymes localized preferentially in COPII vesicles and at the trans-Golgi. Shortly after heparin treatment, the HS-modifying enzyme moved from cis to trans-Golgi, which coincided with increased HS sulfation. Finally, it was shown that COPI subunits and Sec24 gene expression changed. Collectively, these findings demonstrate that knowledge of the ER-Golgi dynamics of HS-modifying enzymes via

vesicular trafficking is a critical prerequisite for the complete delineation of HS biosynthesis.

**Key words:** Biosynthesis, heparan sulfate, COPI, COPII, Golgi apparatus

## 1. Introduction

Protein glycosylation, the post-translational modification of proteins in which carbohydrate moieties are conveniently attached, by either by N- or O-linkages, is a new frontier in the field of glycomics (Martin et al., 2009). One form of post-translational modification, O-Glycosylation, involves attachment of sugars to serine and threonine and plays a vital role in protein function (Haltiwanger & Lowe, 2004).

Heparan sulfate (HS) is a sulfated glycosaminoglycan (GAG) found on the cell membrane and in the extracellular matrix throughout the animal kingdom (Cássaro & Dietrich, 1977; G. F. Medeiros et al., 2000). Alongside heparin (Hep), HS is a member of the GAG family which are present in tissues as proteoglycans, where the polysaccharide chains are O-linked to a protein backbone. Their chains are mainly composed of repeating disaccharide units of 1,4 linked uronate, either  $\beta$ -D-glucuronate or  $\alpha$ -L-iduronate, and  $\alpha$ -D-glucosamine, where N-acetyl-D-glucosamine residues become de-N-acetylated and N-sulfated, then, some of the  $\beta$ -D-glucuronates undergo epimerization at C5 to  $\alpha$ -L-iduronates. Furthermore, sulfate groups may be added at C2 of the uronate residues, C6 of the glucosamine residues and, less commonly, at C3 of the glucosamine residues (Dietrich, Nader, & Straus, 1983; Meneghetti et al., 2015). These structural modifications are the result of a series of enzymatic

reactions that do not, however, result in complete substitution throughout the HS chains, and this results in complex substitution patterns.

A central hypothesis in the field is that the HS chain substitution pattern encodes its capability to influence many key biological processes (Cavalheiro et al., 2017; Moreira et al., 2004; Nader et al., 1999; Sarrazin, Lamanna, & Esko, 2011) through interactions with hundreds of proteins (Nunes et al., 2019). It is now appreciated that there exists complex and regulated biosynthetic machinery capable of producing finely-tuned HS structures and that the heterogeneity characteristic of this system will affect networks of proteins, and eventually, become evident in biological terms.

Template driven biosynthesis is employed for nucleic acids and proteins, but the biosynthesis of HS exhibits no analogous system. Models of HS-modifying enzymes form complexes and act collectively (Pinhal et al., 2001; Presto et al., 2008; Victor et al., 2009), and reactions being carried out in a hierarchical order (Esko & Selleck, 2002; Lindahl, 1977) have been proposed. Models have been advanced that are able to explain the relative abundance of both common and uncommon structures (Meneghetti et al., 2017; Rudd & Yates, 2012). Furthermore, it has been shown that the localization of EXT1/EXT2 (Exostosin-1/Exostosin-2) in distinct Golgi cisternae modulates the synthesis of HS (Chang et al., 2013), suggesting that vesicular trafficking could play an important role in the regulation of HS biosynthesis. Hence, the interrogation of cargo sorting, vesicle assembly and trafficking that takes place to deliver GAG biosynthetic enzymes throughout the ER and Golgi, may be necessary for the complete description of HS biosynthesis and the success of subsequent structure and function studies.

In the present study, the influence of vesicular trafficking mediated by COPI and COPII in the distribution of HS-modifying enzymes along the early secretory pathway of relevance to the regulation of HS biosynthesis has been evaluated. Furthermore, the effect of pharmacological agents that are known to inhibit vesicular trafficking and alter HS synthesis were explored. This study sheds light on how the natural Golgi influences the biosynthesis of HS.

## 2. Material and methods

### 2.1 Reagents and antibodies

G418 disulfated salt solution was purchased from Sigma Aldrich (Saint Louis, MO, USA). Brefeldin A solution (1000X) (BFA) was obtained from Invitrogen (San Diego, CA, USA). Heparin (Hep) from porcine mucosa was a kind gift of Extrasul (Jaguapitã, PR, Brazil).  $\text{H}_2^{35}\text{SO}_4$  carrier free was purchased from National Centre for Nuclear Research Radioisotope POLATOM (Otwock, Poland). Mouse antibodies to HS3ST1 (B01P) and HS3ST3A1 (B01P) were obtained from Abnova (Taipei, Taiwan), antibodies to C5-epimerase and Golgin97 from Abcam (Cambridge, MA, USA) and antibody to NDST1 (M01) from Abgent (San Diego, CA, USA). Rabbit antibodies to anti- $\alpha$ -COP,  $\beta$ -COP and GM130 were purchased from Abcam, antibodies to COPII (Sec23) and HS3ST5 from Thermo Scientific (Rockford, IL, USA) and antibody to HS2ST (N-term) from Abgent. Goat antibody to GFP (I-16) was obtained from Santa Cruz Biotechnology (Dallas, TX, USA). Secondary antibodies conjugated to Alexa Fluor<sup>®</sup> 488, Alexa Fluor<sup>®</sup> 633 and Alexa Fluor<sup>®</sup> 647 were purchased from Thermo Fisher Scientific. Information regarding all these antibodies is specified in table S2.

## 2.2 Cell culture

Endothelial cells derived from human umbilical vein endothelial cells were maintained in F12 medium supplemented with 10% (v/v) fetal bovine serum (FBS, Cultilab, Campinas, Brazil), penicillin (100 U/mL) and streptomycin (100 µg/mL) (Gibco, CA, USA) at 37 °C in a humidified atmosphere of 2.5% CO<sub>2</sub>. At 80–85% confluence, the cells were detached with a solution of pancreatin (2.5%) diluted 1:10 (v/v) in EBSS, collected by centrifugation, suspended in F12 medium as described above (Buonassisi & Venter, 1976).

## 2.3 Transfection and expression of HS3ST5 in culture

For cell transfection, EC cells were plated at  $5 \times 10^4$  cells per well (500 µL) in 24-well plates and transfected with 550 ng of cDNA coding HS3ST5, cloned into the vector pAcGFP-N1 (Clontech plasmid PT3716-5), using transfection FuGENE HD<sup>®</sup> reagent at a ratio 5:1, according to the manufacturer's instructions (Promega Corporation, WI, USA). The transfected cells (EC-HS3ST5) were cultured in the presence of G418 disulfated salt (0.5 µg/mL) and selected in accordance to the level of HS3ST5 expression.

## 2.4 Flow cytometry

EC and EC-HS3ST5 post-confluent cells ( $1 \times 10^6$ ) were detached from the plate using EDTA 500 µM in PBS solution. The cells were washed with PBS, fixed with 2% paraformaldehyde in PBS for 30 min and then permeabilized with 0.01% saponin in PBS for 30 min. After, the cells were incubated with primary antibody for 2 h, followed by incubation with fluorescent-

labeled secondary antibody for 40 min. The antibodies were diluted in PBS containing 1% BSA. Data were collected using the FACSCalibur flow cytometer (Becton Dickinson, Franklin Lakes, USA) and data analyses were performed using FlowJo v.10 software (Tree Star Inc, Ashland, USA).

## **2.5 Capillary-like tube formation**

EC cells ( $5 \times 10^4$  cells) were seeded in 96-well plates, previously incubated with reconstituted basement membrane (Matrigel™, BD Biosciences, USA), in 200  $\mu$ L of F12 medium containing 10% SFB and incubated at 37 °C, 2.5% CO<sub>2</sub> for 24 hours. The capillary-like vascular structures were analyzed in an Axio Observer.A1 microscope equipped with AxioCam MRc and AxioVision software (Carl Zeiss).

## **2.6 Immunofluorescence and confocal microscopy**

EC and EC-HS3ST5 cells were seeded on 13 mm coverslips placed in 24-well plate ( $1 \times 10^4$  cells/coverslip). After 4 days, the medium of transfected cells was removed, and the cells treated with BFA (3  $\mu$ g/mL) for 2 h or with heparin (20  $\mu$ g/mL) for 1, 2, 3 or 4 h. The cells were then washed thrice with phosphate-buffered saline (PBS), fixed with 2% paraformaldehyde in PBS solution for 30 min at room temperature and washed with 0.1 M glycine. Afterwards, coverslips were sequentially incubated with blocking solution (0.02% saponin, 1% BSA in PBS solution, 30 min) and primary antibodies for 2 h. For visualization of tagged HS3ST5, the recombinant enzyme was stained with antibody against GFP in order to increase the signal. After washing with PBS, the cells were incubated with the appropriate fluorescent-labeled

secondary antibodies for 1 h at room temperature. All antibodies were diluted in blocking solution. Once the first label was completed, labeling for the second protein was performed similarly. Nuclei were stained with 4',6-diamidino-2-phenylindole (DAPI, Thermo Fischer Scientific, 1 µg/ml in blocking buffer). Lastly, coverslips were mounted on glass microscope slides using a mounting medium (Fluoromount-G, Birmingham, AL, USA) and fluorescence images were captured on a Leica TCS SP8 CARS confocal microscope (Wetzlar, Germany) with HC PL APO 63x/1.40 oil immersion objectives. The images represent the sum slides projections corresponding to the z-series of confocal stacks. Negative controls, prepared without primary antibody, were used for background correction. Two independent experiments were performed for each cell condition.

The fluorescence images were quantified using the Leica LAS X Life Science software (Leica Microsystems) and colocalization intensity was expressed according to Pearson correlation values. These coefficients measure the linear trend of an association between two variables, as well as the direction of the relationship. The coefficients lie between -1 and 1 and specific values measure of the strength of the relationship between variables. Coefficient values between 0 and 1 indicate positive linear correlation (Schober, Boer, & Schwarte, 2018). These values were obtained in Leica LAS X Life Science software.

## **2.7 Super-Resolution Ground State Depletion (SR-GSD) Microscopy**

Transfected cells were seeded on 18 mm high precision round coverslips (Paul Marienfeld GmbH & Co. KG, Lauda-Königshofen, Germany) placed in 12-

well plate ( $2 \times 10^4$  cells/coverslip). After 3 days, the cells were washed thrice with iced PBS and fixed in two steps. Initially, cells were treated with buffer A (5 mM EGTA, 5 mM  $MgCl_2$ , 5 mM glucose, 10 mM MES, 150 mM NaCl) containing 0.3% glutaraldehyde and 0.01% saponin for 2 min at room temperature and, then, with 0.5% glutaraldehyde diluted in buffer A for 10 min at room temperature. After washing, the cells were treated with 0.1%  $NaBH_4$  in PBS for 7 min at room temperature, washed and incubated with blocking solution (0.1% saponin, 5% FSB in PBS solution) for 1 h. The cells were then incubated with primary antibodies (1:50, diluted in PBS containing 0.1% saponin and 1% BSA) for 18 h at 4 °C. After washing, the cells were then incubated with appropriate fluorescent-labeled secondary antibodies (1:50, diluted in PBS containing 0.1% saponin and 1% BSA) for 90 min. Once the first label was completed, staining for the second protein was performed similarly. Finally, the coverslips were mounted on depression slides containing embedding medium (70 mM  $\beta$ -mercapto-ethylamine in PBS solution). The images were captured on a Leica SR GSD 3D microscope (Wetzlar, Germany) equipped with a 160x high power super-resolution objective.

## 2.8 Composition analysis of HS disaccharides

Disaccharide composition analysis of HS extracted from transfected cells that had been subjected to Hep stimulation was accomplished by enzymatic degradation followed by liquid chromatography (Vicente, Lima, Nader, & Toma, 2015). Briefly, the transfected cells were subjected to metabolic labeling with carrier free [ $^{35}S$ ]-sulfate (150  $\mu$ Ci/ml) in serum-free F12 medium for 18 h at 37 °C in an atmosphere containing 2.5%  $CO_2$ . Heparin (20  $\mu$ g/mL) was added to

the medium from 1 to 4 h before the end of the radioactive sulfate labeling period since the stimulation of HS synthesis by heparin can be detected immediately after incubation of the cells with heparin (Nader, Buonassisi, Colburn, & Dietrich, 1989) and the ratio of sulfate incorporation in HS chains is constant between 4 and 24h (Sampaio, Dietrich, Colburn, Buonassisi, & Nader, 1992). This approach was used to avoid variations in metabolic labeling periods. After labeling, the culture-conditioned medium was collected, and the cells removed from the plate with 3.5 M urea in 25 mM Tris-HCl pH 8.0. Both cell extract and medium were submitted to proteolysis with maxatase separately (proteolytic enzyme purified from *Bacillus subtilis*) (Biocon, Rio de Janeiro, RJ, Brazil) (4 mg/ml in 50 mM Tris-HCl, pH 8.0 containing 1.5 mM NaCl) at 60 °C. After proteolysis, nucleic acids and peptides were precipitated by the addition of 90% trichloroacetic acid (10% of sample volume), and the GAGs present in the supernatant were precipitated with 3 volumes of iced methanol at -20 °C for 24 h. The precipitates formed (GAGs) were collected by centrifugation (4,000 rpm for 20 min at 4 °C), dried and suspended in 100 µL distilled water. The sulfated GAGs were identified and quantified by agarose gel electrophoresis in PDA buffer (0.05 M 1,3-diaminepropane acetate) (Dietrich & Dietrich, 1976). Lastly, 10,000 cpm of HS were incubated with 40 µL of each heparitinases I and II from *Flavobacterium heparinum* in 20 mM Tris-HCl, pH 7.4 containing 4 mM CaCl<sub>2</sub> e 50 mM NaCl at 30 °C for 18h. The <sup>35</sup>S-labeled degradation products were chromatographed in PhenoSphere™ 5 µM SAX (150 × 4.6 mm), previously calibrated with HS disaccharide standards, using a NaCl gradient (0-1 M) for 30 min at a flow rate of 1 mL/min. Individual fractions (0.3 mL) were collected and counted on a Micro-Beta counter. The Δ-degradation products of

HS were generated for three independent experiments and the products of digestion combined prior to analysis to allow detection. Therefore, the results represent an overall trend and were expressed as monosulfated, disulfated and trisulfated disaccharide groups.

## 2.9 RNA extraction and real-time PCR

Total RNA was extracted from cultured cells using Trizol reagent (Invitrogen, Carlsbad, USA) according to the manufacturer's instructions. RNA extraction was performed for wild type and transfected cells as well as to transfected cells subjected to heparin treatment (20 µg/mL). Reverse transcriptase reaction was performed from 2 µg of total RNA by using ImProm-II™ Reverse Transcription System (Promega). Aliquots of cDNA obtained were amplified in PCR and quantitative real-time PCR reactions, using the primers described in table S3. PCR reactions were performed using Master Mix (2X) (Promega) and carried out at an initial denaturation step of 95 °C for 2 min, followed by 35 cycles of denaturation at 95 °C for 30 s, annealing at 55 °C for 30 s and extension at 72 °C for 2 min, and final extension step at 72 °C for 5 min. The PCR products were analyzed on 1% agarose gels in TAE buffer at 100 V for 30 min. In addition, real-time PCR amplifications were performed using Maxima® SYBER Green Master Mix 2X (Fermentas, Waltham, MA, USA). The reactions were first subjected to an initial denaturation step at 95 °C for 10 min, followed by 40 cycles at 95 °C of 15 s (denaturation step) and at 60 °C for 1 min (annealing /extension steps). Melting curves were generated after the last amplification cycle to assess the specificity of the amplified products. The reactions were performed in triplicate on the 7500 Real Time PCR System

(Applied Biosystems, Beverly, MA, USA). The relative expression levels of genes were calculated using the  $2^{-\Delta Ct}$  method (Livak & Schmittgen, 2001). The transcript of ribosomal protein L13a (RPL13a) was used as a control to normalize the expression of target genes.

## 2.10 Statistical analysis

Results were expressed as the mean  $\pm$  standard deviation of three independent experiments. Statistical analysis was determined by one-way analysis of variance (ANOVA) followed by Turkey test or Student's *t*-tests. The statistical significance of differences was set at  $p < 0.05$ .

## 3. Results

### 3.1 Subcellular localization of fluorescently tagged heparan sulfate 3-O-sulfotransferase 5 (HS3ST5)

3-O-sulfotransferase is believed to be the last enzyme to modify the HS chains according to the classic HS biosynthetic pathway (Esko & Selleck, 2002; Lindahl, 1977). Nevertheless, in a previous study (Meneghetti et al., 2017), it was demonstrated that 3-O-sulfation can occur in what would be considered to be distinct biosynthetic steps according to the latter theory. Owing to these observations, 3-O-sulfotransferase was selected to have its subcellular localization investigated using tagged-expression systems in endothelial cells (EC) (Fig. S1), previously characterized with EC markers (Fig. S2).

The localization of the tagged-protein in the Golgi apparatus and coated vesicles was confirmed by immunostaining. As shown in Fig. 1A, tagged-HS3ST5 colocalized with both GM130, a cis-Golgi protein marker and Golgin97,

a trans-Golgi protein marker confirming its presence in both Golgi cisternae, and highlighting that, regardless of the order in which 3-O-sulfation happens during the hierarchical HS biosynthesis, this enzyme is trafficked continually amongst the different Golgi cisternae. Tagged-HS3ST5 exhibited similar distribution in both COPI, exemplified by  $\alpha$ -COP and  $\beta$ -COP subunits, and COPII vesicles, represented by staining of the Sec23 subunit, further confirming that HS3ST5 is constantly cycled through the ER-Golgi pathway (Fig. 1A). Further analysis was also conducted using super resolution microscopy and the results clearly showed the localization of HS3ST5 in both COPI and II vesicles (Fig. 1B).

### **3.2 Effects of brefeldin A on the localization of HS-modifying enzymes in vesicular trafficking**

Knowing that the tagged-HS3ST5 is distributed across the Golgi and present in both COPI and II vesicles, we then evaluated the localization and influence of vesicular trafficking on the transport of HS-modifying enzymes along the secretory pathway to determine whether HS-modifying enzymes undergo both anterograde and retrograde Golgi transport. To do so, EC-HS3ST5 cells were treated with brefeldin A (BFA), a pharmacological inhibitor of ADP-ribosylation factors, which are responsible for recruitment of COPI subunits (Peyroche et al., 1999). In the presence of BFA, HS3ST5 displayed higher levels of colocalization in COPII vesicles, showing that the enzyme was maintained during anterograde transport (Fig. 1C and D). It is known that BFA causes Golgi cisternae disassembly and the redistribution of proteins from the cis and medial-Golgi into the ER (Lippincott-Schwartz, Yuan, Bonifacino, & Klausner, 1989). As expected, the BFA treatment induced disassembly of the

Golgi indicated by GM130 and Golgin97 scattered staining (Fig. 1C and E). The effect of BFA was also followed by changes in HS3ST5 distribution along the Golgi cisternae from cis- to trans-Golgi (Fig. 1C and E).

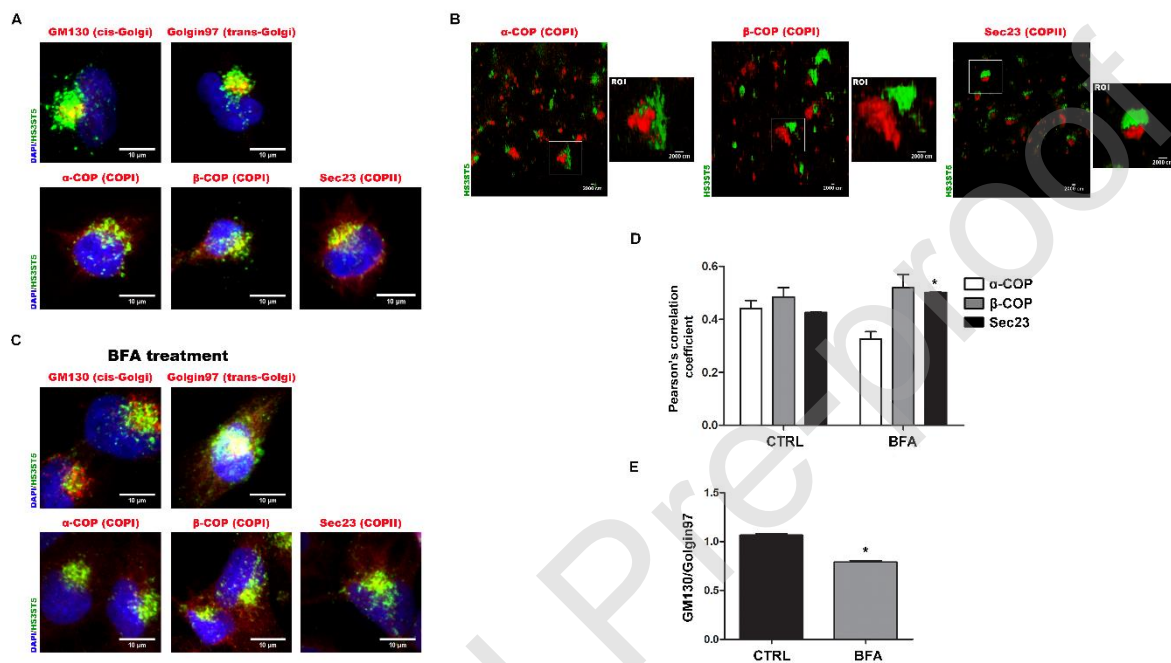


**Fig. 1.** Subcellular localization of fluorescent HS3ST5. (A) Transfected cells were labeled with anti-GFP antibody (tagged HS3ST5, green) and specific antibodies to cis-Golgi (GM130) and trans-Golgi (Golgin97), both in red, or to coated vesicles (red). The staining was revealed with secondary antibodies conjugated with Alexa Fluor® 488 (green) and Alexa Fluor® 633 (red). COPI vesicles were visualized by  $\alpha$ -COP and  $\beta$ -COP staining and COPII vesicles were visualized by Sec23 staining. Scale bars in images: 10  $\mu$ m. (B) Super resolution microscopy images of HS3ST5 (green) and COPI and COPII vesicles (red). Scale bars: 2000 nm. (C) After treatment with BFA (3  $\mu$ g/mL) for 2h, EC-HS3ST5 cells were labeled with anti-GFP (tagged HS3ST5, green) and specific antibodies to GM130 (cis-Golgi) or Golgin97 (trans-Golgi), both in red, or to coated vesicles (red). Pearson's correlation coefficient represents rate of colocalization of recombinant HS3ST5 in coated vesicles (D) and in cis-Golgi (GM130) and in trans-Golgi (Golgin97) (E). Data are presented as mean  $\pm$  standard deviation of three independent experiments. \* $P < 0.05$ , relative to control (One-way ANOVA in (D) and Student's t-test in (E)).

The profile of other HS-modifying enzymes (NDST1, C5-epimerase, heparan sulfate 2-O-sulfotransferase (HS2ST), HS3ST1 and HS3ST3A) in the presence of BFA, relative to HS3ST5, was also analyzed by immunostaining and confocal microscopy. All enzymes presented colocalization with HS3ST5 (Fig. 2), which shows that all HS-modifying enzymes are colocalized at Golgi cisternae and that they are sorted and trafficked by similar mechanisms.

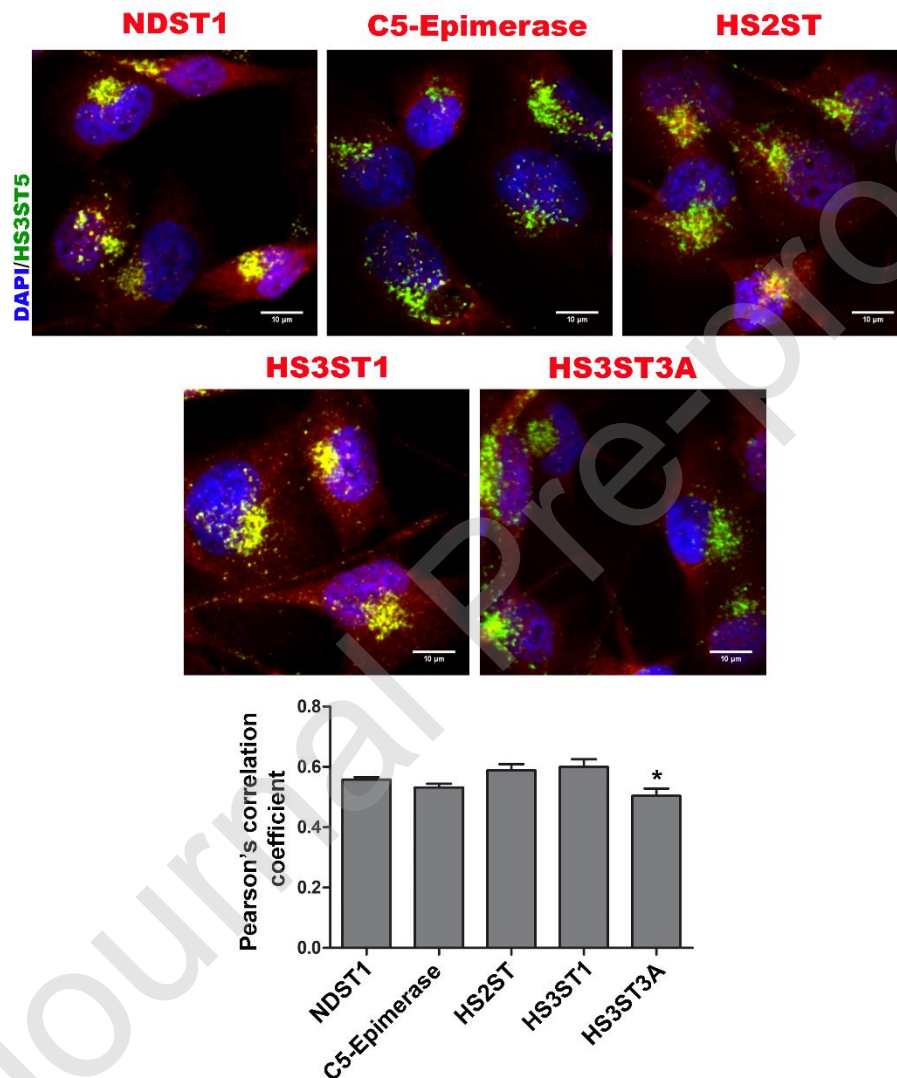


**Fig. 2.** Distribution profile of HS-modifying enzymes following BFA treatment. After treatment with BFA (3 µg/mL) for 2h, EC-HS3ST5 cells were double-labeled for HS3ST5-GFP and HS-modifying enzymes (NDST1, C5-Epimerase, HS2ST, HS3ST1 and HS3ST3A). Secondary antibodies conjugated with Alexa Fluor® 488 (green) and Alexa Fluor® 633 (red), respectively, were used. Scale bars: 10 µm. Pearson's correlation coefficient represents the rate of colocalization of the tagged HS3ST5 with each HS-modifying enzyme. Data are presented as

mean  $\pm$  standard deviation of three independent experiments. \* $P < 0.05$ , relative to HS3ST1 (One-way ANOVA).

### **3.3 Vesicular trafficking and Golgi apparatus localization of HS3ST5 changes with heparin treatment**

It is well known (Nader et al., 1989; Nader, Dietrich, Buonassisi, & Colburn, 1987) that when ECs are exposed to heparin, an upregulation of HS synthesis with increased sulfate levels is observed (Fig. S3 and Table S1). Also, these changes are detected shortly after the treatment and observed to both cell-extracted and secreted HS (Nader et al., 1989; Sampaio et al., 1992) suggesting that they may occur even before *de novo* protein synthesis. The stimulus for the synthesis of HS chains is mediated by the binding of heparin to fibronectin (Trindade, Bouças, et al., 2008; Trindade, Oliver, et al., 2008) leading to integrin activation, which results in the phosphorylation of focal adhesion proteins as well as in the activation of the MAPK kinase pathway (V. P. Medeiros et al., 2012). Owing to these observations, to assess whether this change in HS biosynthesis was the result of changes in HS-modifying enzymes trafficking along the Golgi cisternae, the cells were exposed to heparin and shortly after, the distribution profile of the HS3ST5 relative to coated vesicles and Golgi apparatus was analyzed by confocal microscopy after immunofluorescence staining. There were no changes in HS3ST5 distribution in either COPI or COPII vesicles (Fig. 3) highlighting that both anterograde and retrograde transport are actively engaged in HS-modifying enzymes trafficking. However, changes in HS3ST5 distribution within the different Golgi cisternae were observed (Fig. 4). While the HS3ST5 was preferentially present in the cis-Golgi in cells with no treatment, or during the first hour of heparin exposure,

HS3ST5 changed its favoured distribution from cis to trans-Golgi in subsequent hours (2-3 h).

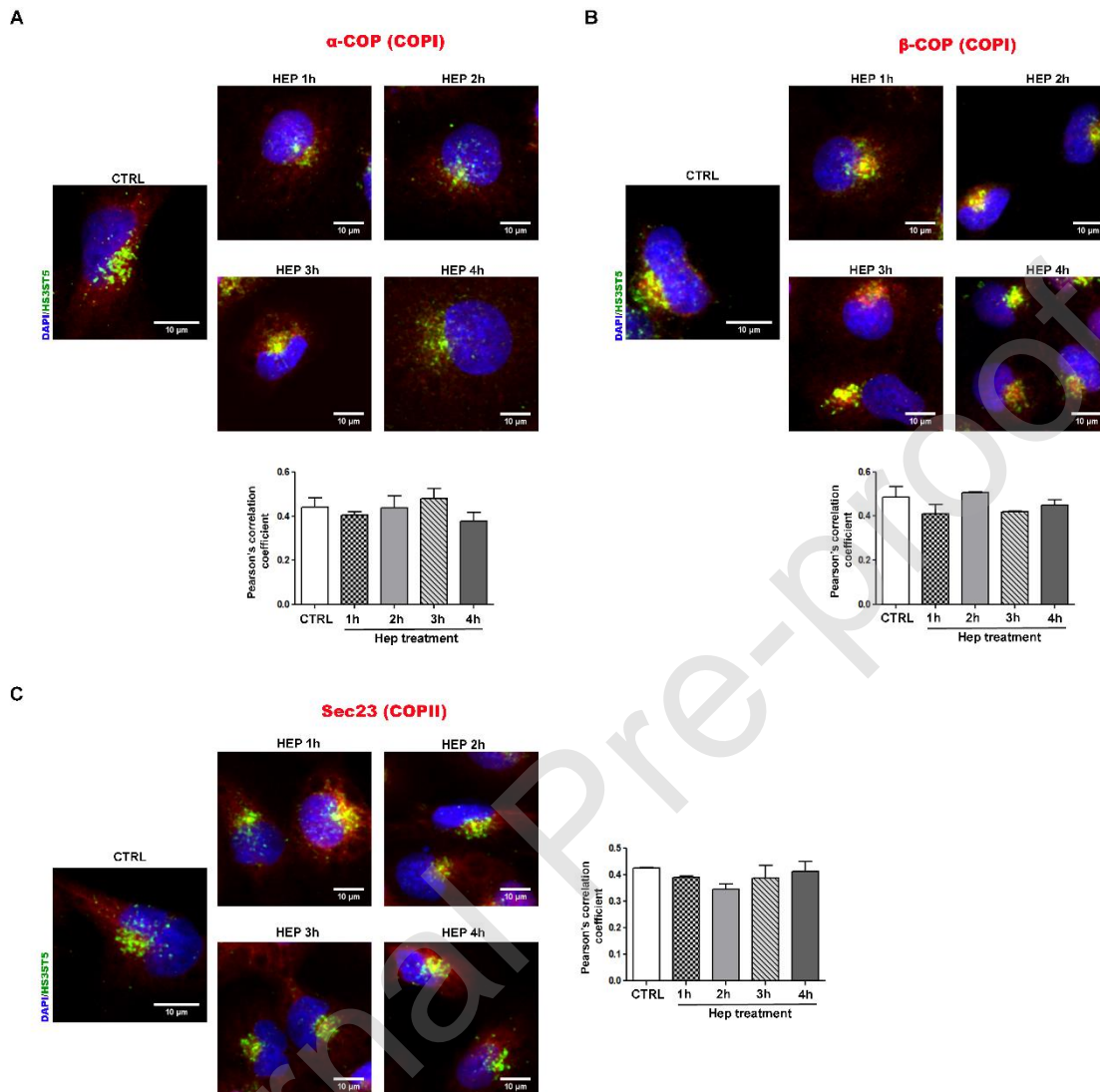


**Fig. 3.** Distribution profile of HS3ST5 in coated vesicles in the presence of heparin. After treatment with heparin (20  $\mu\text{g}/\text{mL}$ ) from 1 to 4 h, EC-HS3ST5 cells were double-labeled with antibodies to GFP (tagged HS3ST5) and  $\alpha$ -COP (A),  $\beta$ -COP (B) or Sec23 (C). The cells were revealed with secondary antibodies conjugated with Alexa Fluor® 488 or Alexa Fluor® 633. Recombinant HS3ST5 and coated vesicles are shown in green and red staining, respectively. Pearson's correlation coefficient represents rate of colocalization of recombinant HS3ST5 in coated vesicles (down and right panels). Scale bars in images: 10  $\mu\text{m}$ .

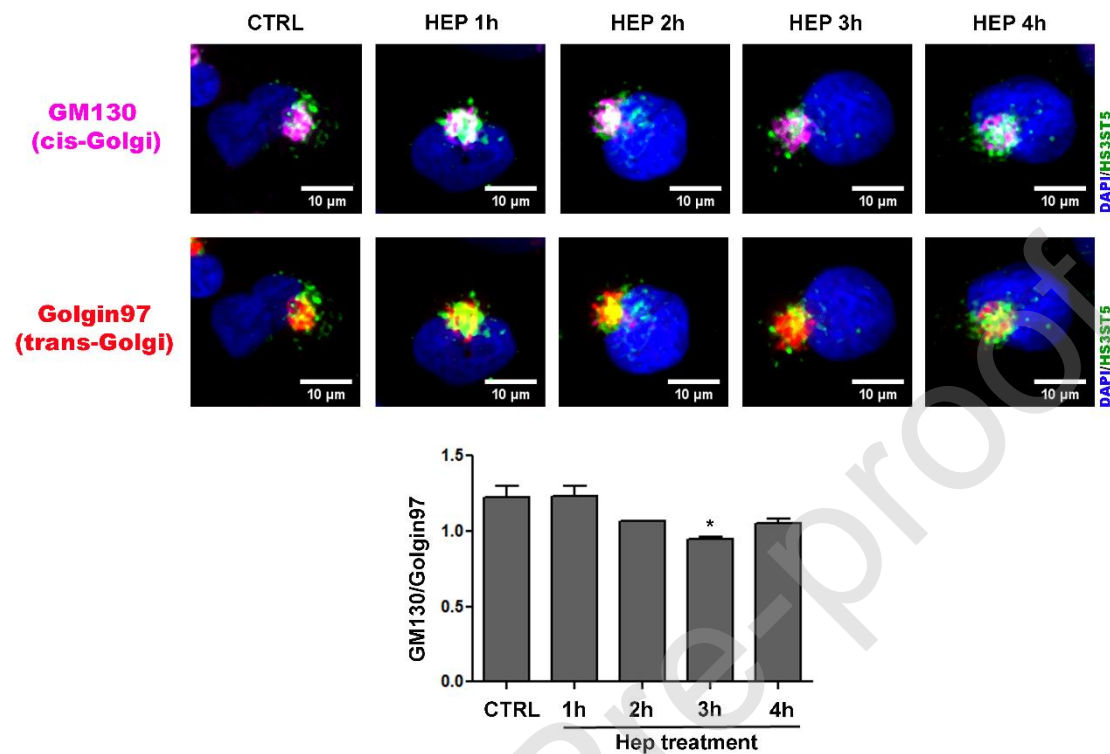
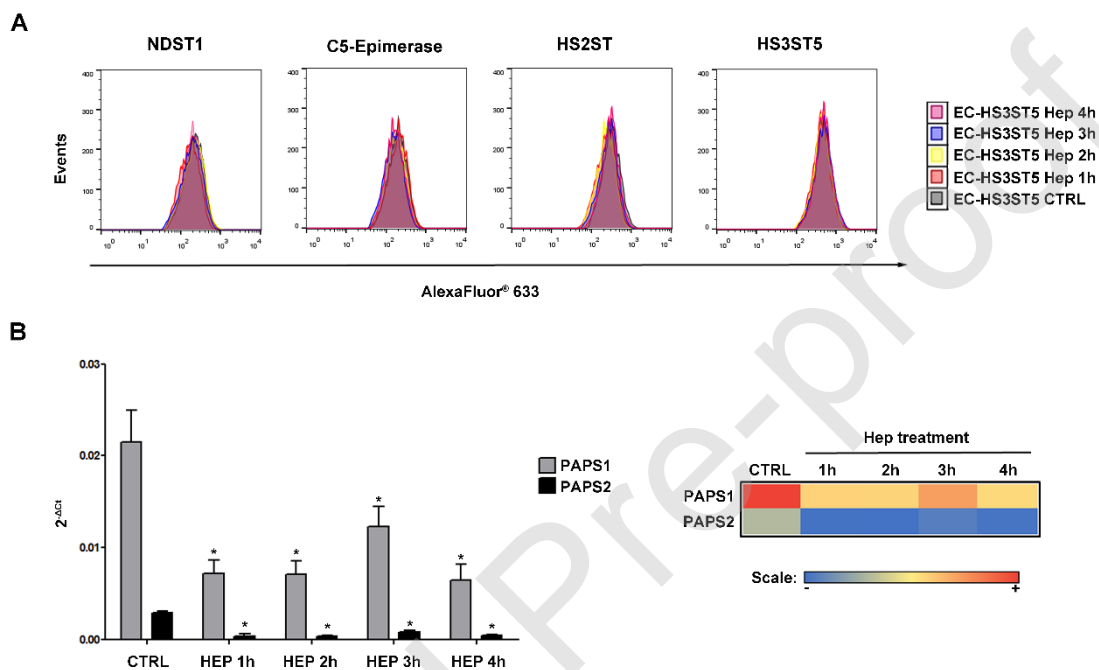


**Fig. 4.** Distribution profile of HS3ST5 in Golgi apparatus following heparin treatment. After treatment with heparin (20 µg/mL) for 1 to 4 h, EC-HS3ST5 cells were triple-staining for GFP (tagged HS3ST5), GM130 (cis-Golgi) and Golgin97 (trans-Golgi). Secondary antibodies conjugated with Alexa Fluor® 488, Alexa Fluor® 594 and Alexa Fluor® 647, respectively were used. Tagged HS3ST5 is shown in green, whereas GM130 and Golgin97 are shown in magenta and red, respectively. The ratio GM130/Golgin97 corresponds to the Pearson's correlation coefficients obtained for the tagged HS3ST5 in the cis-Golgi and in the trans-Golgi, respectively (bottom panel). Scale bars: 10 µm. Data are presented as mean ± standard deviation of three independent experiments. \*P<0.05, relative to control (One-way ANOVA).

### 3.4 HS-modifying enzymes and PAPS synthase levels are not up-regulated following heparin treatment

The changes in HS structure could, however, be the result of the upregulation in sulfotransferase and PAPS synthase expression. To further

confirm our hypothesis that trafficking of HS-modifying enzymes is instead responsible for the detected structural changes, protein and gene expression experiments were conducted. Flow cytometry analysis for specific HS-modifying enzymes (NDST1, C5-Epimerase, HS2ST and HS3ST5) indicated that the protein levels remained unchanged throughout heparin treatment (Fig. 5A). Gene expression analysis also showed significant decrease in both PAPS



synthase isoforms during heparin treatment (Fig. 5B). These results are consistent with the hypothesis that enzyme trafficking, rather than protein/gene expression, regulates HS biosynthesis.

**Fig. 5.** Protein and gene expression of components of HS biosynthesis in presence of heparin. (A) Protein expression of HS-modifying enzymes (NDST1, C5-epimerase, HS2ST and HS3ST5) in transfected cells previously treated with heparin was evaluated by flow cytometry using antibodies specific for each enzyme. Following incubation with primary antibodies, cells were incubated with secondary antibody conjugated with Alexa Fluor® 633 and analyzed by flow cytometry. (B) PAPS synthases mRNA level in EC-HS3ST5 cells treated with heparin was analyzed in real-time. The results were expressed as mean  $\pm$  standard deviation of three experiments. (Right panel) A heat map was generated of mean values obtained in the gene expression assays. High and low expression are shown in red and blue respectively. \* $P < 0.05$ , relative to control (One-way ANOVA).

### 3.5 Changes in coated vesicle component expression after heparin stimulus

Finally, gene expression analysis of COPI subunits, as well as Sec24 subunit isoforms of COPII during heparin stimulation, were performed in order to evaluate the relationship between trafficking of HS-modifying enzymes and the expression of coated vesicle subunits responsible for cargo binding and sorting. It is known that while all seven COPI subunits are engaged in cargo recognition (Arakel & Schwappach, 2018; Watson, Frigerio, Collins, Duden, & Owen, 2004; Yu, Lin, Jin, & Xia, 2009), multiple isoforms of Sec24 are the major cargo binding subunit within the COPII vesicle (Mancias & Goldberg, 2008; Miller, Antony, Hamamoto, & Schekman, 2002). Fig. 6A shows that the gene expression for most COPI subunits comprising both B- and F-subcomplexes, changed after stimulation with heparin. Compared to the controls,  $\beta'$ -COP,  $\beta$ -COP and  $\delta$ -COP subunits showed reduced gene expression in the early stages of treatment, while gene expression of  $\gamma$ 1-COP,  $\gamma$ 2-COP and  $\zeta$ 1-COP only changed later. Whereas the  $\gamma$ -COP1 subunit showed a reduction in its mRNA level in 4 h,  $\gamma$ 2-COP and  $\zeta$ 1-COP presented significant increases in gene expression during this time period;  $\zeta$ -COP1 being the principal COPI subunit experiencing the highest modification in gene expression. As for Sec24, gene expression of only isoforms A and B changed, and reduction in mRNA levels alone during the early phase of heparin stimulus was observed (Fig. 6B).

In summary, the results show that upon heparin treatment, cargo sorting associated proteins have their gene expression altered first, followed by changes in genes that code for coat proteins linked to vesicle trafficking within the Golgi cisternae. Collectively, these results are in agreement with the spatial

and temporal changes observed in the Golgi distribution of HS-modifying enzymes that preceded the biosynthesis of HS with increasing sulfate content.

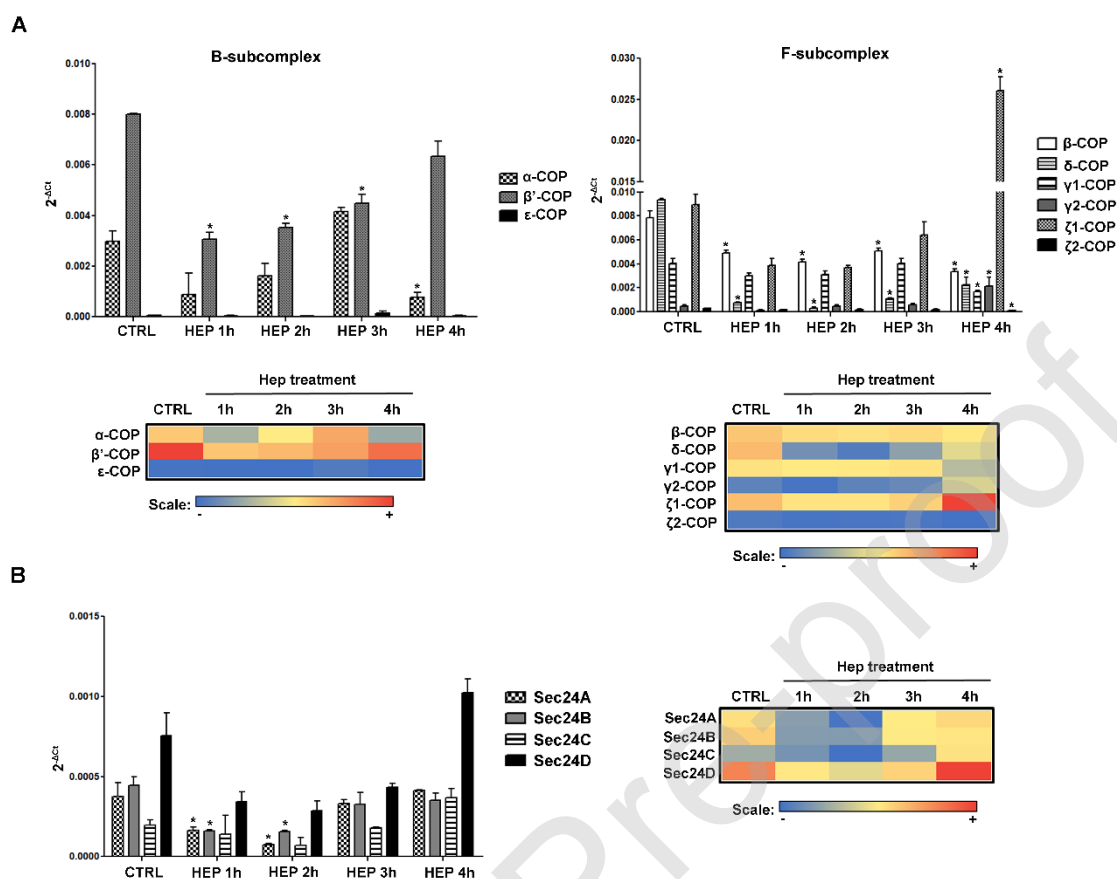


**Fig. 6.** Gene expression of coated vesicles subunits in the presence of heparin. Real-time PCR analysis of COPI subunits subdivided in B- and F-subcomplex (A) and Sec24 subunit (B) in EC-HS3ST5 cells treated with heparin. The results are expressed as mean  $\pm$  standard deviation of three experiments. Heat maps were generated of mean values obtained in the gene expression assays. High and low expression are shown in red and blue respectively. \* $P < 0.05$ , relative to control (One-way ANOVA).

## 4. Discussion

It is clear that the search for the precise control of HS biosynthesis through the modulation of individual enzymes has been unfruitful, while Golgi dynamics remain poorly understood and the different cellular contexts encountered are widely ignored. Artificial Golgi systems have been built as test beds to better understand how the natural Golgi controls the biosynthesis of

GAGs and ultimately, for the design of bioengineered heparin (Martin et al., 2009) but, again, the natural Golgi dynamics and cellular context have not been considered fully. Thus, it seems probable that further regulatory mechanisms are at work; ones that are, perhaps, not apparent at the level of individual biosynthetic enzymes.

The structural diversity of HS could conceivably arise from many cellular events that regulate HS biosynthesis and, consequently, influence HS substitution pattern. The structural variability could, therefore, have been due to UDP-sugar and PAPS availability in Golgi cisternae (Dick, Akslen-Hoel, Grøndahl, Kjos, & Prydz, 2012), the interaction among HS-modifying enzymes themselves and among other proteins (Fang, Song, Lindahl, & Li, 2016; Pinhal et al., 2001; Presto et al., 2008; Senay et al., 2000), as well as their availability and distribution throughout the ER and Golgi. It has been shown, however, that vesicular trafficking influences both spatial and temporal localization of many glycosyltransferases along the ER-Golgi pathway, regulating the sequential order in which these enzymes act during glycoconjugate synthesis (Tu & Banfield, 2010). In the present work, we investigated the influence of the trafficking of HS-modifying enzymes in early secretory pathways at both COPI and COPII vesicles using endothelial cells previously transfected with tagged HS3ST5.

Previous studies have shown that enzymes involved in the glycosylation of proteoglycans display distinct subcellular localization in rat ovarian granulosa cells in the presence of BFA and, whereas the CS/DS-modifying enzymes are exclusively distributed in the trans-Golgi, the HS-modifying enzymes are mainly located in the cis-Golgi (Uhlin-Hansen & Yanagishita, 1993). Nonetheless, other

reports have also demonstrated that N-deacetylase/N-sulfotransferase (NDST) and Heparan sulfate 6-O-sulfotransferase (HS6ST) are localized in the trans-Golgi of endothelial and renal epithelial cells (Humphries, Sullivan, Aleixo, & Stow, 1997; Sampaio et al., 1992), indicating that these differences may reflect dynamism in the localization of HS-modifying enzymes along different Golgi cisternae according to the cellular context. Here, we have shown that HS-modifying enzymes are actively engaged in both anterograde and retrograde Golgi transport and, upon BFA treatment, that HS-modifying enzymes are maintained in anterograde transport, involving COPII vesicles, at the trans-Golgi. Furthermore, regardless of the position in the hierarchical sequence of the biosynthetic process (Esko & Selleck, 2002), enzymes involved in HS biosynthesis (NDST1, C5-Epimerase, HS2ST, HS3ST1 and HS3ST3A) displayed similar localization and distribution, showing that these enzymes were sorted and transported by similar trafficking mechanisms.

Shortly after heparin treatment, the structure of the newly biosynthesized HS is altered (Nader et al., 1989) in ECs. Here, the redistribution of HS3ST5 along the Golgi was observed. Shortly after treatment, the enzyme moved from cis to trans-Golgi, which coincided with the increased HS sulfation levels. These findings show that vesicular trafficking has a role in regulating the transport of HS-modifying enzymes throughout different Golgi compartments and that, eventually, this leads to the synthesis of different HS structures. Consequently, as shown previously for mucin O-glycosylation (Gill, Chia, Senewiratne, & Bard, 2010), depending on cellular context, substitution pattern may be changed following the redistribution of Golgi-resident proteins. This hypothesis was further confirmed by the expression analysis of HS-modifying enzymes, for

which no significant changes in expression were observed. An increase in sulfate levels due to increased levels of PAPS synthase, could also have been expected, but this was not the case. Finally, changes in gene expression of COPI subunits and Sec24 gene expression, which relates to COPII vesicles, were observed which shows that changes in cargo sorting, followed by vesicular assembly and trafficking alter the dynamics of HS-modifying enzymes across the ER and Golgi, and that these changes lead to altered HS structure. Undoubtedly, HS-modifying enzyme trafficking rather than protein upregulation is responsible for the observed changes in HS biosynthesis.

Studies in both yeast and mammalian cells have identified active recycling of Golgi-resident glycosyltransferases through the ER-Golgi pathway mediated by coated vesicles (Gill et al., 2010; Liu, Doray, & Kornfeld, 2018; Storrie et al., 1998; Todorow, Spang, Carmack, Yates, & Schekman, 2000). The different localization of these enzymes in the secretory pathway allows newly synthesized glycoconjugates to encounter glycosyltransferases in a non-uniform distribution to perform glycosylation (Emr et al., 2009; Puthenveedu & Linstedt, 2005) without the need for any *de novo* protein synthesis allowing rapid biosynthesis modulation (Grant & Donaldson, 2009) and, in the case of HS biosynthesis, rapid fine-tuning in HS structure. Mechanisms involved in HS-modifying enzymes retention and trafficking through different compartments and within distinct Golgi cisternae may ensure the production of a wide structural variety of compounds, a key characteristic of these molecules, and may reflect the complexity of glycoconjugate synthesis. While the recycling of some cis-Golgi resident proteins is dependent on direct interaction with the COPI subunits, other Golgi resident enzymes have been shown to require COPI

specific adaptors such as Golgi phosphoprotein 3 (GOLPH3) (Chang et al., 2013; Eckert et al., 2014; Liu et al., 2018). In addition, the retention of glycosyltransferases in the Golgi may also result from protein-protein interactions, protein affinity for the lipid compartment, as well as the composition and size of the transmembrane domain (Patterson et al., 2008; Welch & Munro, 2019) which may also be the case of HS-modifying enzymes.

## 5. Conclusion

Here, active trafficking has been demonstrated for HS-modifying enzymes where changes in their distribution correlated with the synthesis of a more sulfated HS chain. Collectively, the results show that cargo sorting, vesicular assembly and trafficking mediated by COPI and COPII regulate HS biosynthesis by controlling the spatial and temporal distribution of HS-modifying enzymes on different Golgi cisternae. These findings illustrate that HS-modifying enzyme trafficking is a critical prerequisite for the complete delineation of HS biosynthesis and the success of further structure and function studies.

### CRedit authorship contribution statement

**Maria C.Z. Meneghetti:** Methodology, Investigation, Writing - original draft, Writing - review & editing. **Paula Deboni:** Investigation. **Carlos M.V. Palomino:** Investigation. **Luiz P. Braga:** Investigation. **Renan P. Cavaleiro:** Investigation. **Gustavo M. Viana:** Investigation. **Edwin A. Yates:** Conceptualization, Writing - review & editing, Supervision. **Helena B. Nader:** Methodology, Writing - review & editing, Resources, Supervision, Funding

acquisition. **Marcelo A. Lima:** Conceptualization, Methodology, Writing - review & editing, Resources, Supervision, Project administration, Funding acquisition.

### Declaration of Competing Interest

The authors declare no competing financial interests.

### Acknowledgements

The work was supported by grants from Fapesp (Fundação de Amparo à Pesquisa do Estado de São Paulo, 2015/03964-6; 2017/14179-3); CAPES (Coordenação de Aperfeiçoamento de Pessoal de Nível Superior; 0599/2018) and CNPq (Conselho Nacional do Desenvolvimento Científico e Tecnológico; 442357/2014-1).

### References

- Arakel, E. C., & Schwappach, B. (2018). Formation of COPI-coated vesicles at a glance. *J Cell Sci*, 131(5).
- Buonassisi, V., & Venter, J. C. (1976). Hormone and neurotransmitter receptors in an established vascular endothelial cell line. *Proc Natl Acad Sci U S A*, 73(5), 1612-1616.
- Cavalheiro, R. P., Lima, M. A., Jarrouge-Bouças, T. R., Viana, G. M., Lopes, C. C., Coulson-Thomas, V. J., . . . Nader, H. B. (2017). Coupling of vinculin to F-actin demands Syndecan-4 proteoglycan. *Matrix Biol*, 63, 23-37.
- Chang, W. L., Chang, C. W., Chang, Y. Y., Sung, H. H., Lin, M. D., Chang, S. C., . . . Chou, T. B. (2013). The Drosophila GOLPH3 homolog regulates the biosynthesis of heparan sulfate proteoglycans by modulating the retrograde trafficking of exostosins. *Development*, 140(13), 2798-2807.
- Cássaro, C. M., & Dietrich, C. P. (1977). Distribution of sulfated mucopolysaccharides in invertebrates. *J Biol Chem*, 252(7), 2254-2261.
- Dick, G., Akslen-Hoel, L. K., Grøndahl, F., Kjos, I., & Prydz, K. (2012). Proteoglycan synthesis and Golgi organization in polarized epithelial cells. *J Histochem Cytochem*, 60(12), 926-935.
- Dietrich, C. P., & Dietrich, S. M. (1976). Electrophoretic behaviour of acidic mucopolysaccharides in diamine buffers. *Anal Biochem*, 70(2), 645-647.
- Dietrich, C. P., Nader, H. B., & Straus, A. H. (1983). Structural differences of heparan sulfates according to the tissue and species of origin. *Biochem Biophys Res Commun*, 111(3), 865-871.

- Eckert, E. S., Reckmann, I., Hellwig, A., Röhling, S., El-Battari, A., Wieland, F. T., & Popoff, V. (2014). Golgi phosphoprotein 3 triggers signal-mediated incorporation of glycosyltransferases into coatomer-coated (COPI) vesicles. *J Biol Chem*, 289(45), 31319-31329.
- Emr, S., Glick, B. S., Linstedt, A. D., Lippincott-Schwartz, J., Luini, A., Malhotra, V., . . . Wieland, F. T. (2009). Journeys through the Golgi--taking stock in a new era. *J Cell Biol*, 187(4), 449-453.
- Esko, J. D., & Selleck, S. B. (2002). Order out of chaos: assembly of ligand binding sites in heparan sulfate. *Annu Rev Biochem*, 71, 435-471.
- Fang, J., Song, T., Lindahl, U., & Li, J. P. (2016). Enzyme overexpression - an exercise toward understanding regulation of heparan sulfate biosynthesis. *Sci Rep*, 6, 31242.
- Gill, D. J., Chia, J., Senewiratne, J., & Bard, F. (2010). Regulation of O-glycosylation through Golgi-to-ER relocation of initiation enzymes. *J Cell Biol*, 189(5), 843-858.
- Grant, B. D., & Donaldson, J. G. (2009). Pathways and mechanisms of endocytic recycling. *Nat Rev Mol Cell Biol*, 10(9), 597-608.
- Haltiwanger, R. S., & Lowe, J. B. (2004). Role of glycosylation in development. *Annu Rev Biochem*, 73, 491-537.
- Humphries, D. E., Sullivan, B. M., Aleixo, M. D., & Stow, J. L. (1997). Localization of human heparan glucosaminyl N-deacetylase/N-sulphotransferase to the trans-Golgi network. *Biochem J*, 325 ( Pt 2), 351-357.
- Lindahl, U. (1977). Biosynthesis of heparin and heparan sulfate. *Ups J Med Sci*, 82(2), 78-79.
- Lippincott-Schwartz, J., Yuan, L. C., Bonifacino, J. S., & Klausner, R. D. (1989). Rapid redistribution of Golgi proteins into the ER in cells treated with brefeldin A: evidence for membrane cycling from Golgi to ER. *Cell*, 56(5), 801-813.
- Liu, L., Doray, B., & Kornfeld, S. (2018). Recycling of Golgi glycosyltransferases requires direct binding to coatomer. *Proc Natl Acad Sci U S A*, 115(36), 8984-8989.
- Livak, K. J., & Schmittgen, T. D. (2001). Analysis of relative gene expression data using real-time quantitative PCR and the 2(-Delta Delta C(T)) Method. *Methods*, 25(4), 402-408.
- Mancias, J. D., & Goldberg, J. (2008). Structural basis of cargo membrane protein discrimination by the human COPII coat machinery. *EMBO J*, 27(21), 2918-2928.
- Martin, J. G., Gupta, M., Xu, Y., Akella, S., Liu, J., Dordick, J. S., & Linhardt, R. J. (2009). Toward an artificial Golgi: redesigning the biological activities of heparan sulfate on a digital microfluidic chip. *J Am Chem Soc*, 131(31), 11041-11048.
- Medeiros, G. F., Mendes, A., Castro, R. A., Baú, E. C., Nader, H. B., & Dietrich, C. P. (2000). Distribution of sulfated glycosaminoglycans in the animal kingdom: widespread occurrence of heparin-like compounds in invertebrates. *Biochim Biophys Acta*, 1475(3), 287-294.
- Medeiros, V. P., Paredes-Gamero, E. J., Monteiro, H. P., Rocha, H. A., Trindade, E. S., & Nader, H. B. (2012). Heparin-integrin interaction in endothelial cells: downstream signaling and heparan sulfate expression. *J Cell Physiol*, 227(6), 2740-2749.

- Meneghetti, M. C., Hughes, A. J., Rudd, T. R., Nader, H. B., Powell, A. K., Yates, E. A., & Lima, M. A. (2015). Heparan sulfate and heparin interactions with proteins. *J R Soc Interface*, 12(110), 0589.
- Meneghetti, M. C. Z., Gesteira Ferreira, T., Tashima, A. K., Chavante, S. F., Yates, E. A., Liu, J., . . . Lima, M. A. (2017). Insights into the role of 3-O-sulfotransferase in heparan sulfate biosynthesis. *Org Biomol Chem*, 15(32), 6792-6799.
- Miller, E., Antony, B., Hamamoto, S., & Schekman, R. (2002). Cargo selection into COPII vesicles is driven by the Sec24p subunit. *EMBO J*, 21(22), 6105-6113.
- Moreira, C. R., Lopes, C. C., Cuccovia, I. M., Porcionatto, M. A., Dietrich, C. P., & Nader, H. B. (2004). Heparan sulfate and control of endothelial cell proliferation: increased synthesis during the S phase of the cell cycle and inhibition of thymidine incorporation induced by ortho-nitrophenyl-beta-D-xylose. *Biochim Biophys Acta*, 1673(3), 178-185.
- Nader, H. B., Buonassisi, V., Colburn, P., & Dietrich, C. P. (1989). Heparin stimulates the synthesis and modifies the sulfation pattern of heparan sulfate proteoglycan from endothelial cells. *J Cell Physiol*, 140(2), 305-310.
- Nader, H. B., Chavante, S. F., dos-Santos, E. A., Oliveira, T. W., de-Paiva, J. F., Jerônimo, S. M., . . . Dietrich, C. P. (1999). Heparan sulfates and heparins: similar compounds performing the same functions in vertebrates and invertebrates? *Braz J Med Biol Res*, 32(5), 529-538.
- Nader, H. B., Dietrich, C. P., Buonassisi, V., & Colburn, P. (1987). Heparin sequences in the heparan sulfate chains of an endothelial cell proteoglycan. *Proc Natl Acad Sci U S A*, 84(11), 3565-3569.
- Nunes, Q. M., Su, D., Brownridge, P. J., Simpson, D. M., Sun, C., Li, Y., . . . Fernig, D. G. (2019). The heparin-binding proteome in normal pancreas and murine experimental acute pancreatitis. *PLoS One*, 14(6), e0217633.
- Patterson, G. H., Hirschberg, K., Polishchuk, R. S., Gerlich, D., Phair, R. D., & Lippincott-Schwartz, J. (2008). Transport through the Golgi apparatus by rapid partitioning within a two-phase membrane system. *Cell*, 133(6), 1055-1067.
- Peyroche, A., Antony, B., Robineau, S., Acker, J., Cherfils, J., & Jackson, C. L. (1999). Brefeldin A acts to stabilize an abortive ARF-GDP-Sec7 domain protein complex: involvement of specific residues of the Sec7 domain. *Mol Cell*, 3(3), 275-285.
- Pinhal, M. A., Smith, B., Olson, S., Aikawa, J., Kimata, K., & Esko, J. D. (2001). Enzyme interactions in heparan sulfate biosynthesis: uronosyl 5-epimerase and 2-O-sulfotransferase interact in vivo. *Proc Natl Acad Sci U S A*, 98(23), 12984-12989.
- Presto, J., Thuveson, M., Carlsson, P., Busse, M., Wilén, M., Eriksson, I., . . . Kjellén, L. (2008). Heparan sulfate biosynthesis enzymes EXT1 and EXT2 affect NDST1 expression and heparan sulfate sulfation. *Proc Natl Acad Sci U S A*, 105(12), 4751-4756.
- Puthenveedu, M. A., & Linstedt, A. D. (2005). Subcompartmentalizing the Golgi apparatus. *Curr Opin Cell Biol*, 17(4), 369-375.
- Rudd, T. R., & Yates, E. A. (2012). A highly efficient tree structure for the biosynthesis of heparan sulfate accounts for the commonly observed

- disaccharides and suggests a mechanism for domain synthesis. *Mol Biosyst*, 8(5), 1499-1506.
- Sampaio, L. O., Dietrich, C. P., Colburn, P., Buonassisi, V., & Nader, H. B. (1992). Effect of monensin on the sulfation of heparan sulfate proteoglycan from endothelial cells. *J Cell Biochem*, 50(1), 103-110.
- Sarrazin, S., Lamanna, W. C., & Esko, J. D. (2011). Heparan sulfate proteoglycans. *Cold Spring Harb Perspect Biol*, 3(7).
- Schober, P., Boer, C., & Schwarte, L. A. (2018). Correlation Coefficients: Appropriate Use and Interpretation. *Anesth Analg*, 126(5), 1763-1768.
- Senay, C., Lind, T., Muguruma, K., Tone, Y., Kitagawa, H., Sugahara, K., . . . Kusche-Gullberg, M. (2000). The EXT1/EXT2 tumor suppressors: catalytic activities and role in heparan sulfate biosynthesis. *EMBO Rep*, 1(3), 282-286.
- Storrie, B., White, J., Röttger, S., Stelzer, E. H., Sukanuma, T., & Nilsson, T. (1998). Recycling of golgi-resident glycosyltransferases through the ER reveals a novel pathway and provides an explanation for nocodazole-induced Golgi scattering. *J Cell Biol*, 143(6), 1505-1521.
- Todorow, Z., Spang, A., Carmack, E., Yates, J., & Schekman, R. (2000). Active recycling of yeast Golgi mannosyltransferase complexes through the endoplasmic reticulum. *Proc Natl Acad Sci U S A*, 97(25), 13643-13648.
- Trindade, E. S., Bouças, R. I., Rocha, H. A., Dominato, J. A., Paredes-Gamero, E. J., Franco, C. R., . . . Nader, H. B. (2008). Internalization and degradation of heparin is not required for stimulus of heparan sulfate proteoglycan synthesis. *J Cell Physiol*, 217(2), 360-366.
- Trindade, E. S., Oliver, C., Jamur, M. C., Rocha, H. A., Franco, C. R., Bouças, R. I., . . . Nader, H. B. (2008). The binding of heparin to the extracellular matrix of endothelial cells up-regulates the synthesis of an antithrombotic heparan sulfate proteoglycan. *J Cell Physiol*, 217(2), 328-337.
- Tu, L., & Banfield, D. K. (2010). Localization of Golgi-resident glycosyltransferases. *Cell Mol Life Sci*, 67(1), 29-41.
- Uhlin-Hansen, L., & Yanagishita, M. (1993). Differential effect of brefeldin A on the biosynthesis of heparan sulfate and chondroitin/dermatan sulfate proteoglycans in rat ovarian granulosa cells in culture. *J Biol Chem*, 268(23), 17370-17376.
- Vicente, C. M., Lima, M. A., Nader, H. B., & Toma, L. (2015). SULF2 overexpression positively regulates tumorigenicity of human prostate cancer cells. *J Exp Clin Cancer Res*, 34, 25.
- Victor, X. V., Nguyen, T. K., Ethirajan, M., Tran, V. M., Nguyen, K. V., & Kuberan, B. (2009). Investigating the elusive mechanism of glycosaminoglycan biosynthesis. *J Biol Chem*, 284(38), 25842-25853.
- Watson, P. J., Frigerio, G., Collins, B. M., Duden, R., & Owen, D. J. (2004). Gamma-COP appendage domain - structure and function. *Traffic*, 5(2), 79-88.
- Welch, L. G., & Munro, S. (2019). A tale of short tails, through thick and thin: investigating the sorting mechanisms of Golgi enzymes. *FEBS Lett*.
- Yu, W., Lin, J., Jin, C., & Xia, B. (2009). Solution structure of human zeta-COP: direct evidences for structural similarity between COP I and clathrin-adaptor coats. *J Mol Biol*, 386(4), 903-912.

Journal Pre-proof